Available online at www.sciencedirect.com
SCIENCE DIRECT®
Cement and Concrete Research 36 (2006) 663 – 670
Cement and Concrete Research

The application of Raman spectrometry to the investigation of cement Part II: A micro-Raman study of OPC, slag and fly ash

S.S. Potgieter-Vermaak [a,*,1], J.H. Potgieter [b], M. Belleil [c], F. DeWeerdt [d], R. Van Grieken [a]

[a] Department of Chemistry, University of Antwerp, Universiteitsplein 1, B-2610, Antwerp, Belgium
[b] School of Chemical And Metallurgical Engineering, University of the Witwatersrand, Private Bag X3, Wits, 2050, South Africa
[c] Renishaw, 15 rue Albert Einstein, Champs-sur-Mame, 77437 Mame La Vallèe Cedex 2, France
[d] Hoge Raad voor Diamant (HRD), 22 Hovenierstraat, B-2018, Antwerp, Belgium

Received 21 March 2005; accepted 22 September 2005

Abstract

Various attempts to use Raman spectrometry to analyse the mineral phases in hydrated and unhydrated cement have been made and results were published on pure synthesized mineral phases as early as 1976. Limited investigations were reported in the past three decades on pure mineral cement phases, white cement and ordinary Portland cement (OPC) analysed with visible (VIS) excitation at 514.5 and 632 nm (mainly with normal Raman spectrometry) and near-infrared (NIR) excitation at 1064 nm (mainly Fourier Transform Raman Spectrometry — FT–Raman). Results were distinctly different for VIS and NIR lasers. Newman and co-workers assigned these differences to a fluorescence phenomenon. Previous work on the characterization of secondary cement materials (SCMs) by means of Raman spectrometry is even more limited. This work focused on the characterization of OPC, fly ash and slag, using ultraviolet–visible (UV–VIS), VIS and NIR excitation in micro-Raman spectrometry and the results obtained for OPC and fly ash will be compared with previously published results.

Keywords: UV–VIS; VIS; NIR Raman spectrometry; Cement; Fly ash; Slag; Characterization

1. Introduction

The mineral cement phases alite (C_3S), belite (C_2S) and tricalcium aluminate (C_3A) in its pure form and as it is present in cement have been investigated since 1976 up to the present and results regarding their respective characteristic Raman scattering have been published [1–5]. In a recent review article [6], these results were discussed and it was found that the results obtained with NIR FT–Raman and VIS Raman spectrometry were distinctly and consistently different for the calcium silicate phases. It was shown by Newman et al. [2] that contrary to the rule, 1064 nm excitation produces structural fluorescence effects, masking the true Raman scattering observed with VIS Raman spectrometry. The absence of corresponding anti-Stokes shifts in the Raman spectra obtained with 1064 nm excitation proved its fluorescent origin. On the other hand the confirmation of Raman shifts for the mineral phases with the use of two different visible excitation sources (541.5 and 632.8 nm), proved that the Stokes spectra obtained were indeed due to Raman scattering. No real evidence of the cause of fluorescence experienced with 1064 nm excitation was reported in any of the papers. Both Newman et al. [2] and Dyer and Hendra [5] tried to prove that the presence of rare earth elements (REE) in the cement could be the culprit, but did not succeed. The spectra of the calcium aluminate phases on the other hand, were comparable and seem to be independent of laser excitation wavelength. The use of Raman spectrometry on grey cements is reported not to be routinely successful and further investigation into the use of different lasers was advised.

Fly ash is the residue from the burning of pulverized coal in thermal power stations. It consists of a variety of different particle size fractions of hollow silica alumina glass spheres with average sizes ranging from 5 to 45 μm, after classification. Fly ash has a number of useful applications that serves to utilize some of the

* Corresponding author. Tel.: +32 3 8202346; fax: +32 3 8202376.
E-mail address: sanja.potgieter@ua.ac.be (S.S. Potgieter-Vermaak).
[1] Permanently employed by the Department of Chemistry and Physics, Faculty of Natural Sciences, Tshwane University of Technology, Pretoria, South Africa.

0008-8846/$ - see front matter © 2005 Published by Elsevier Ltd.
doi:10.1016/j.cemconres.2005.09.010

large amounts being produced. The bulk of current consumption of fly ash going worldwide is as an extender in cement and concrete [7]. The characterization of fly ash by means of Raman spectrometry has not been cited in the technical literature recently and the only reference to Raman analysis and fly ash is found in articles written by Scheetz et al. [8,9]. The intimate mixture of multiphases, resulting in a largely heterogeneous material, and the fact that fly ash is intrinsically a rather weak Raman scatterer, make it a difficult material to study. What is more, the intensities of the scans are further influenced by the significant light scattering that occurs from the small particles that are interfaced with air. Scheetz characterized fly ash using 514.5 nm excitation and a micro-Raman configuration. He and his co-workers identified and characterized both the crystalline and amorphous glassy phases. The crystalline components of fly ash are thermal products of the original inorganic compounds in the coal. The most common crystalline phase is quartz, followed by anhydrite, gypsum, calcium silicates and aluminates. Scheetz and White [8] did not succeed in detecting hematite and any of the iron-spinels. The glassy phases have been characterized as high silica glass that gives a broad inelastic scattering at 1050–1100 cm^{-1} and calcium aluminate glass with a scattering at 700–750 cm^{-1} [9].

Slag, an almost fully non-crystalline glassy material, is a by-product from the steel-making industry and granulated blast furnace slag is often used as an extender in cement due to its latent hydraulic properties. These hydraulic activities are influenced by the properties of the slag, including the glass content, chemical and mineralogical composition. Technical literature regarding the determination of the mineralogical composition by means of Raman spectrometry is limited and it is usually determined by X-ray diffraction (XRD). Typical compositions, as supplied in the open technical literature, indicate that they consist of various iron oxides, such as magnesioferrite, magnetite and hematite; silicates, such as larnite, belite and bredigite (calcium silicates), merwinite ($Ca_3MgSi_2O_8$) and gehlenite ($Ca_2Al_2SiO_7$) and finally, oxides, such as birnessite and groutellite (manganese oxides). Some of these minerals have been well characterized with Raman spectroscopy and reported in the technical literature, but no literature could be traced where these have been identified in slag by means of Raman spectrometry.

This paper describes the investigation conducted and the results obtained on OPC, fly ash Class F and an iron blast furnace slag, using UV–VIS, VIS and NIR laser excitation sources in a micro-Raman configuration.

2. Experimental procedure

2.1. Materials

The cement analysed was an OPC, with a typical elemental analysis as given in Table 1. The blast furnace slag was obtained from Slagment (Pty) Ltd and was produced as a by-product from steel manufactured by Iscor (Pty) Ltd, Gauteng Province, RSA. The fly ash used was from Ash Resources (Pty) Ltd, and was recovered from the Lethabo Power Station, Gauteng Province, RSA. The two fly ash samples used in this study were classified as a Class F fly ash and had average particle sizes of 5 and 15 μm, respectively. All the samples were put in a solid sample holder where a small amount was compacted together to give a smooth surface and no further sample preparation was necessary.

Table 1
Chemical composition of the materials (%wt)

Element (expressed as %wt oxide)	Cement	Fly ash	Slag
SiO_2	21.9	52.6	37
Al_2O_3	4.3	34.6	14
Fe_2O_3	2.1	3.2	
Mn_2O_3	0.9	<0.1	
TiO_2	0.3	1.7	
CaO	62.6	4.1	34
MgO	4.2	1.1	12
SO_3	2.2	0.7	0.9 (S)
P_2O_5	<0.1	0.3	<0.1
Cl	<0.1	<0.1	
K_2O	0.7	0.6	0.8
Na_2O	0.1	0.2	
LOI	0.4	0.8	
Blaine fineness (m^2/kg)	310	1300	350
Total	99.7	99.9	98.7

2.2. Instrumentation

Micro-Raman Spectrometry provided information about the chemical composition and identity of the sample. The different materials were examined with a Renishaw InVia micro-Raman spectrometer coupled with a Peltier cooled CCD detector. Excitation was provided by both the 514.5 and 785 nm lines of a continuous wave 25 mW Ar^+ and 300 mW diode array lasers, respectively. Samples were scanned using a syncro scan mode from 100 to 4000 cm^{-1} at a spectral resolution of about 2 cm^{-1}. The acquisition time for each scan varied from 10 to 40 s, to obtain the best condition for the spot analysed. The number of accumulations varied from 3 to 10, which were summed, in order to provide a better signal-to-noise ratio. Spectra were obtained using 50× or 20× magnification objectives. Calibration was done by using the 520.5 cm^{-1} line of a silicon wafer. Multiple spot analyses on different areas of the samples were performed to ensure representative results. Data acquisition was carried out with the Spectracalc software package GRAMS (Galactic Industries, Salem, NH, USA). Spectra were not corrected for background. The UV–VIS excitation was done by using a Renishaw RM 2000 instrument in combination with a 325 nm laser line of a 25 mW HeCd laser. The UV grating (2400 g mm^{-1}) is blazed at 400 nm with a dispersion of approximately 2 cm^{-1} in the measured range. The objective is an Olympus NUV 15× UV objective. The laser line is removed with an edge filter, with a cut-off at approximately 580 cm^{-1} from the laser line.

3. Results and discussion

3.1. OPC measurements

The results of the measurements done on the OPC sample with the UV–VIS, VIS and NIR lasers are depicted in Fig. 1.

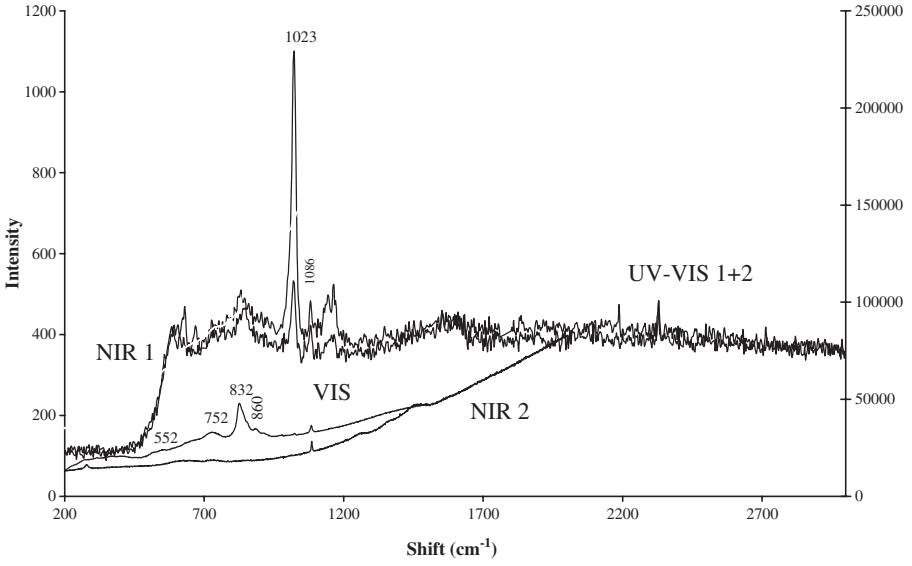

Fig. 1. Comparison of the Raman shifts observed with UV–VIS, VIS and NIR excitation of OPC.

The spectra in Fig. 1 illustrate the general results obtained when the instrument was used in a scanning mode ranging from 100 to 2000 cm^{-1}. Instrument settings regulate an exposure time of minimum 10 s in such cases. The v_1 SiO_4 stretching vibrations at 832 cm^{-1} are clearly noted in the spectra of all three excitation sources, indicating that it is a true Raman shift observed and is indicative of the presence of the alite mineral phase, as reported by Conjeaud et al. [3]. The v_1 SiO_4 stretching vibration of the belite phase, as reported by Conjeaud and Boyer [3] at 860 cm^{-1}, was only observed with the NIR laser. The bending mode of the silicate is not always observed and gives a broad shift from 525 to 550 cm^{-1} with 514 and 785 nm excitation. It was not observed with the UV–VIS excitation since its cut off wave number is at 500 cm^{-1}. The presence of gypsum and calcium carbonate was identified with all the lasers. The v_1 and v_4 vibrations of the carbonate were observed at 1084 and 712, respectively, and the lattice vibration at 280 cm^{-1}. The gypsum was identified as calcium sulphate dihydrate by the symmetric vibration of the sulphate ion observed at 1007 cm^{-1}, as well as the anhydrite at 1023 cm^{-1}.

Static scans were also performed with the NIR excitation and the results are shown in Fig. 2a. With the static scan it was possible to expose the sample for a shorter time, with a minimum of 1 s, and the power delivered at the sample could be increased significantly to improve S/N. Using this mode of measurement a limited spectral range could be scanned. The broad weak signals that could be otherwise observed as illustrated in Fig. 2b, could be enhanced and thus the anti-Stokes inelastic scattering could verify the validity of the observed shift. From Fig. 2a it can be seen that the main shifts designated to alite and belite in OPC are well observed with the NIR laser and is also reflected in the anti-Stokes spectrum. It is often seen that the two shifts present themselves as one broadband, and wave numbers ranging from 824 to 860 cm^{-1} were observed. The average maximum intensity for what is perceived to be the alite mineral phase is at 831 cm^{-1} and the one definite belite response was identified at 859 cm^{-1}. It is difficult to designate the shifts to either alite or belite, as identified by Dyer [5] at 848 and 860 cm^{-1} for belite and for the alite shifts, at 845 and 832 cm^{-1} and it is therefore concluded that mixtures of alite and belite are detected. The extended scans for VIS excitation had a good signal to noise ratio and static scans were not required. Nevertheless, anti-Stokes spectra were obtained and the results for VIS spectra are shown in Fig. 3. From Fig. 3 it can be seen that the main shifts designated to alite and belite in OPC are well observed with the VIS laser and is also reflected in the anti-Stokes spectrum. The Stokes and anti-Stokes shifts are slightly shifted in comparison with those observed with NIR. The alite v_1 SiO_4 shifts is assigned at an average of 828 cm^{-1} and the corresponding shift for belite at 840 cm^{-1}. A broad shift ranging from 720 to 748 cm^{-1} with an average highest intensity at 730 cm^{-1} could be the result of the presence of a tricalcium aluminate phase, the presence of ferric ions and/or the v_4 CO_3 vibration of the carbonate ion. The presence of calcite, gypsum and anhydrite is also observed as in the case of the NIR spectra.

3.2. Fly ash measurements

The Raman spectra collected at selected points on the classified 5 μm fly ash, using the 514.5 nm laser as excitation source, are illustrated in Fig. 4. Various crystalline and glassy mineral phases were detected. In most of the spectra the presence of elemental carbon is observed, as indicated by the Raman shifts at 1353 cm^{-1} and 1603 cm^{-1}, which is characteristic of the G (graphite) and D (disordered) modes commonly found in elemental carbons. The fundamental G peak normally dominates at 1585 cm^{-1} for poly-crystalline graphite and shifts to a superimposed single feature at about 1600 cm^{-1} for small disordered graphitic structures, while the D band is caused by defects in the graphitic layers and will consequently become stronger with the presence of amorphous

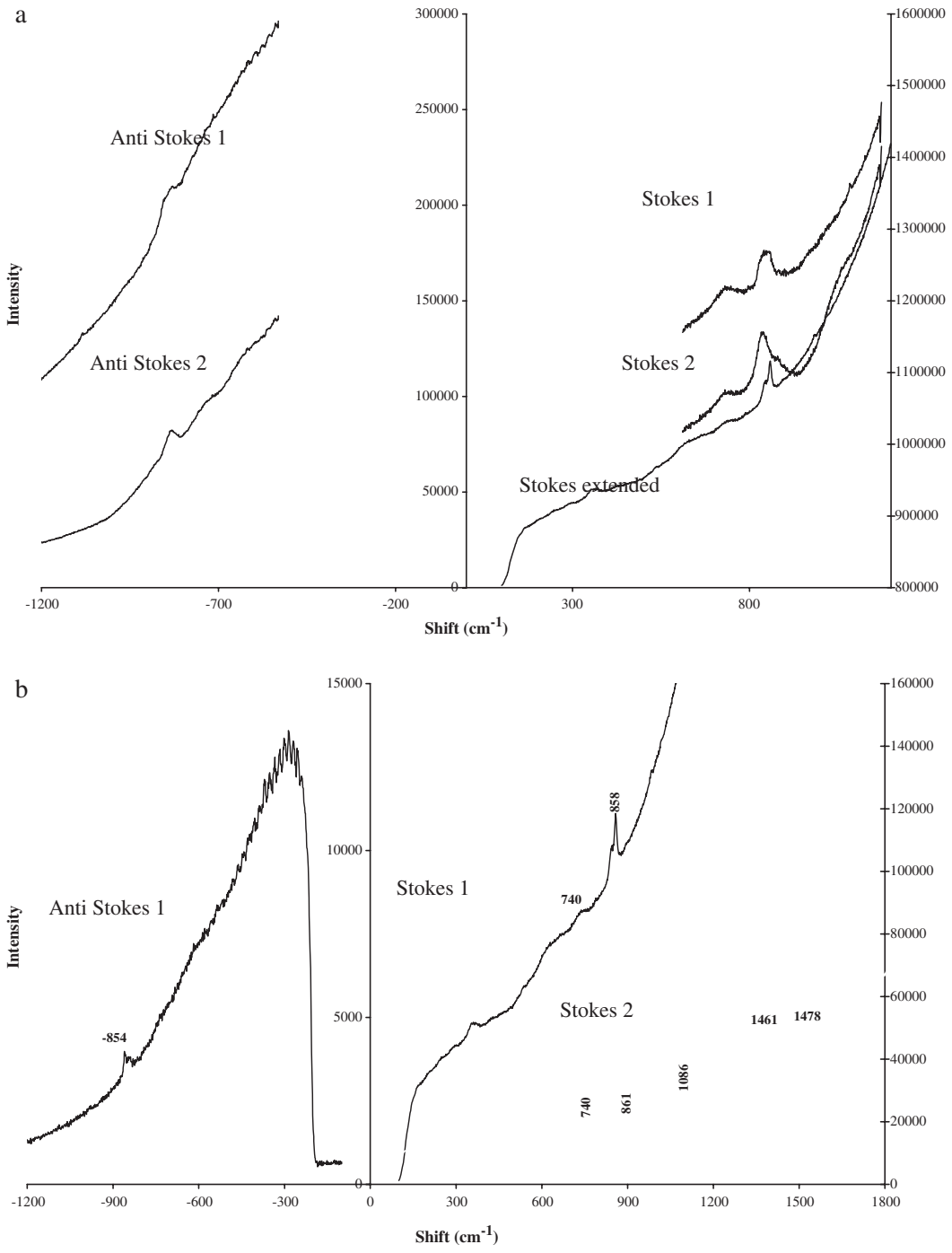

Fig. 2. (a) Stokes and anti-Stokes spectra of OPC obtained with static scans using the 785 nm laser. (b) Stokes and anti-Stokes spectra of OPC obtained with extended scans using the 514.5 nm laser.

carbon. The presence of these shifts was not exclusive to the commonly found discrete black particles, but was also often observed with the bulk of the particles. Quartz also frequents the spectra; it was mostly associated with darker coloured particles. Similar to the observation made by Scheetz and White [8], most of the well-known Raman shifts are very weak except for the strongest symmetric vibration at 461 cm^{-1}. The second most commonly occurring crystalline phase is anhydrite, according to Sheetz and White [8], and it was certainly observed in various points analysed. The strongest inelastic scattering of the sulphate ion is observed at 1016 cm^{-1}. Contrary to the work of Scheetz and White [8], various iron-containing minerals could be detected in this investigation. A number of spinels such as magnesioferrite and iron chromite with typical Raman shifts at 709, 484, 343, 724, and 537 cm^{-1}, respectively, were identified. Pyrite (FeS) and pyrhotite (Fe_xS) were also identified and were associated with discrete dark red and brown particles. A typical spectrum for pyrhotite is given in Fig. 4. Iron oxides have also been detected, such as magnetite, as illustrated in Fig. 4. Evidence of tricalcium

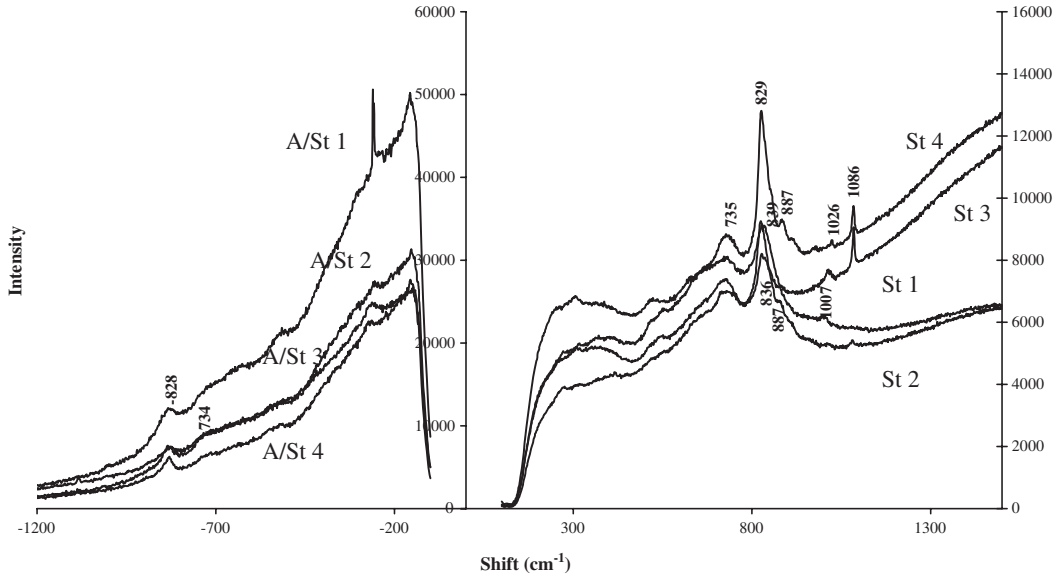

Fig. 3. Stokes and anti-Stokes spectra of OPC obtained with static scans using the 514.5 nm laser.

silicate (C_3S) is indicated by the typical shift at around 840 cm^{-1} as depicted in Fig. 4. Evidence of dicalcium silicates was not observed.

The glassy phases can be characterized as calcium aluminate or high silicate glasses, according to Scheetz [9]. The spectra obtained with the 514.5 nm laser were certainly more sensitive to the crystalline phases than the 785 nm spectra. The so-called high silicate glasses are observed in some of the spectra at around 1080 cm^{-1} and the calcium aluminate glassy phase between 700 and 750 cm^{-1}.

The NIR excitation was performed on a classified fly ash with an average particle size less than 15 μm. It is evident from Fig. 5a that the carbon inclusions have a significant amount of amorphous carbon and this was mostly associated with discreet black particles. The bulk of the samples were difficult to analyse due to the small spherical nature of the particles interfaced with air and consequent difficulty in focusing of the laser beam. The spectra in Fig. 5a are representative of the bulk of the sample and indicate the presence of amorphous carbon, quartz, anhydrite, C_3S and calcium aluminate glass phase, the latter identified by the very broad shift around 730 cm^{-1}. Identification of other species is impeded by the large amount of fluorescence. Discrete dark red particles have been unambiguously identified as an iron sulphide species with shifts at 295.7, 412.8 and 228.7 cm^{-1} as the main modes, as depicted in Fig. 5b. Orange-brown areas, also located distinctly

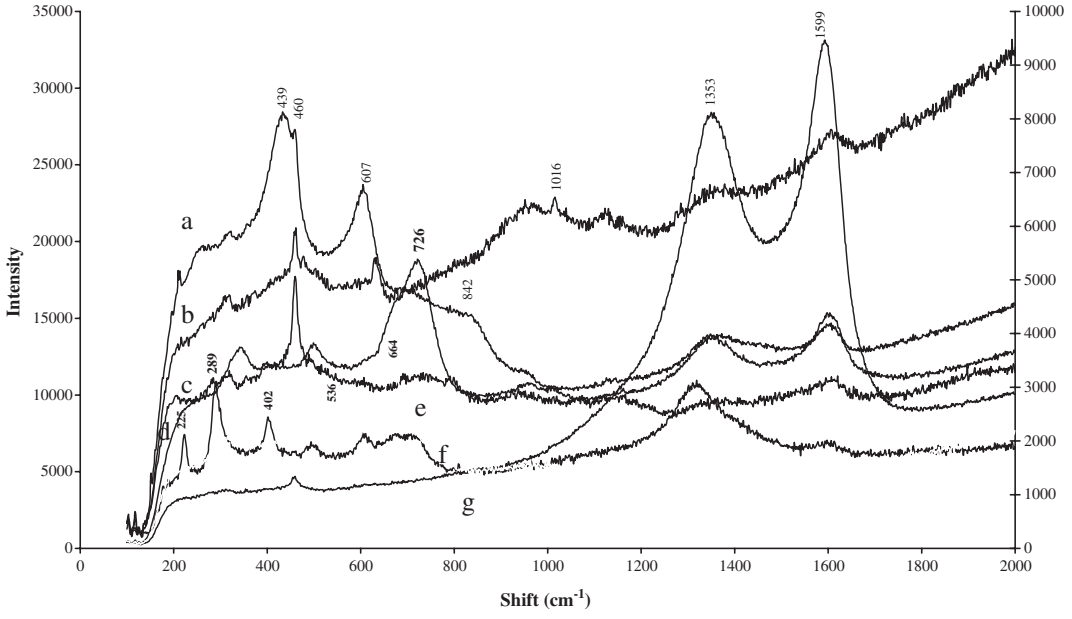

Fig. 4. Raman spectra of classified fly ash obtained with the 514.5 nm excitation. a=Q-C-R; b=anhydrite-CS glass; c=S glass-Q; d=Fe_xS; e=$Fe(III)Fe(II)O_4$; f=Fe_xS; g=C; Q=quartz; R=rutile; C=carbon; Anhyd=anhydrite; S glass=silicate glass.

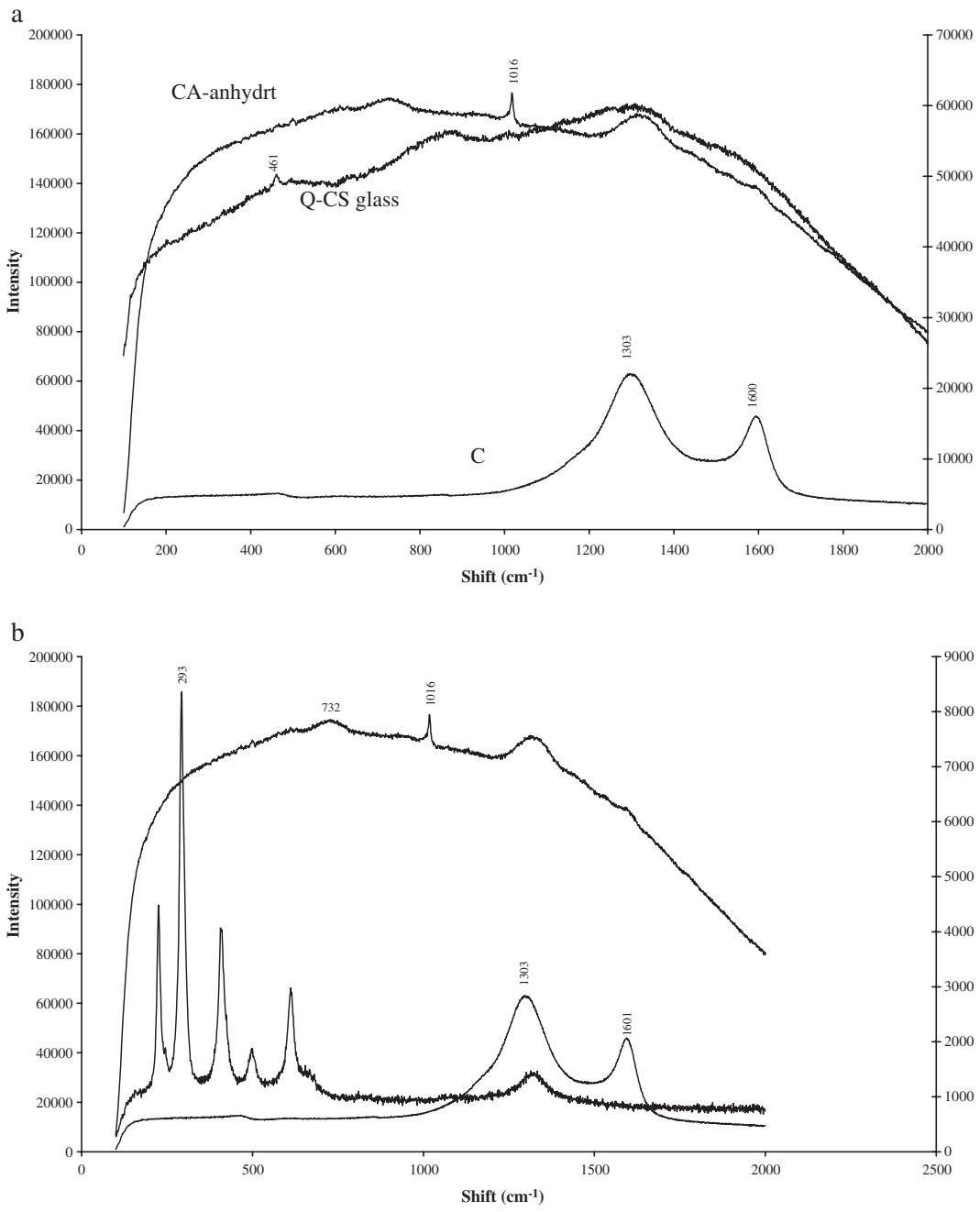

Fig. 5. (a) Raman spectra obtained of classified fly ash with the 785 nm excitation. (b) Raman spectra obtained of classified fly ash with the 785 nm excitation indicating the presence of pyrite. CA=calcium aluminate; CS glass=calcium silicate glass.

in the samples, were identified as a sulphate species due to the identification of a shift at 1005 cm^{-1}, which corresponds well to the vibration expected for the symmetrical O–S–O stretching of an iron sulphate species (not shown).

3.3. Slag measurements

The slag sample was considerably more difficult to analyse due to a large fluorescent background observed with all lasers. The best excitation wavelength was found to be 514.5 nm. With the UV–VIS excitation no spectra could be obtained. The VIS spectra had a smaller fluorescence background and especially the darker particles could be analysed with good spectral resolution. The dark red and black particles proved to be discreet in distribution and spectra obtained were either pure graphitic carbon or iron compounds, or both. The G and D bands have been assigned at 1593 and 1353 cm^{-1} respectively. The iron compounds found were various iron oxides such as hematite, and the presence of iron sulphide was also observed.

The presence of calcium silicates was also discerned, as described by Kirkpatrick et al. [10]. Si–O symmetric stretchings were observed at 893–909 cm^{-1} with a shoulder at 980 cm^{-1} suggesting Q^1 and Q^2 tetrahedra. An Si–O–Si bending

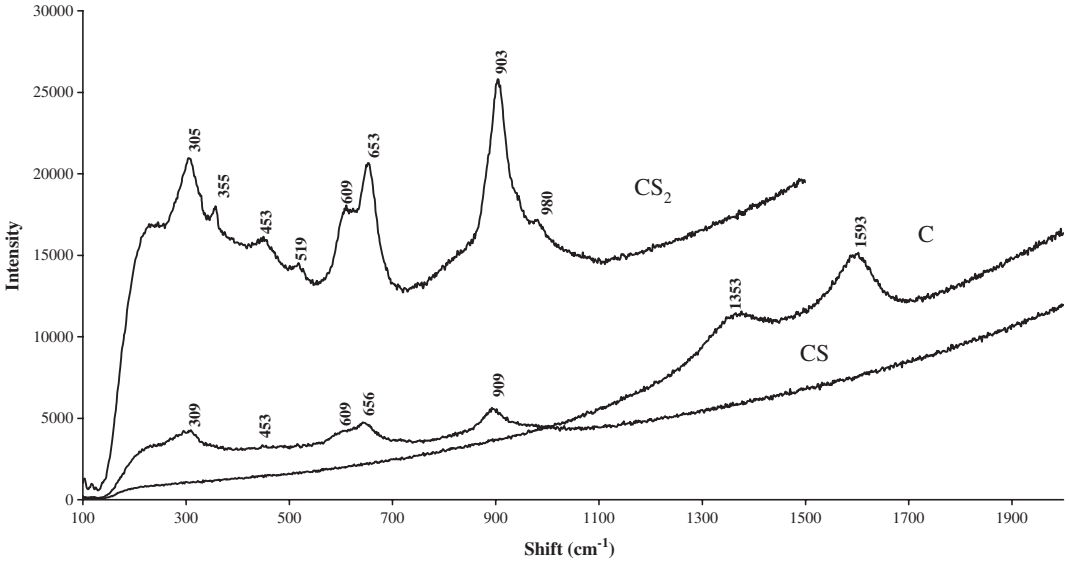

Fig. 6. Raman spectra of blast furnace slag obtained with the 514.5 nm excitation. CS=calcium silicate; CS2=calcium silicate 2nd spectrum.

at 656 cm^{-1} indicates a Q^2 tetrahedron. An OH translation at 309 cm^{-1} due to vibrations involving Ca–O polyhedra was also detected. The bending mode is frequented by a shoulder on the lower wave number side, typically at 609 cm^{-1} and could be assigned to Q^3 tetrahedral bending motions, although the typical Si–O stretching and Si–O–Si bending modes for Q^3 tetrahedra have not been observed. The presence of these vibrational modes has been confirmed by determining the anti-Stokes inelastic scattering. Fig. 6 illustrates some of the typical spectra observed for slag using the VIS excitation source. These spectra resemble those obtained for low calcium binary $CaO–SiO_2$ systems studied by Kalampounias et al. [11]. The resemblance fitted best with $xCaO–(1-x)SiO_2$ glasses for $0.3 \leq x \leq 0.45$.

The compounds identified by means of NIR excitation were very similar to those obtained by VIS excitation. The darker particles proved to be either graphitic carbon or iron-related compounds as illustrated in Fig. 7. Iron compounds were once again mixtures of various iron hydroxides and some iron sulphides. In contrast to the observed calcium silicates using the 514.5 nm excitation, no silicates were identified due to huge fluorescence phenomena.

The suggested calcium–silicates and calcium–magnesium–silicates were not identified specifically, and although the presence of a calcium–silicate has been confirmed, it could not be assigned to specific mineral phases. It was noted, however, that spectra obtained for melilite by Fredericci et al. [12] in a study of the crystallization mechanism and properties of a blast furnace slag, were in close resemblance to the CS(2) spectrum in Fig. 6. The study was done with a micro-Raman configuration and VIS excitation. Melilite is a solid solution between akermanite ($2CaO·MgO·2SiO_2$) and gehlenite ($2CaO·Al_2O_3·2SiO_2$) and main shifts have been reported by Fredericci et al. at 912, 661 and 626 cm^{-1}. The spectrum

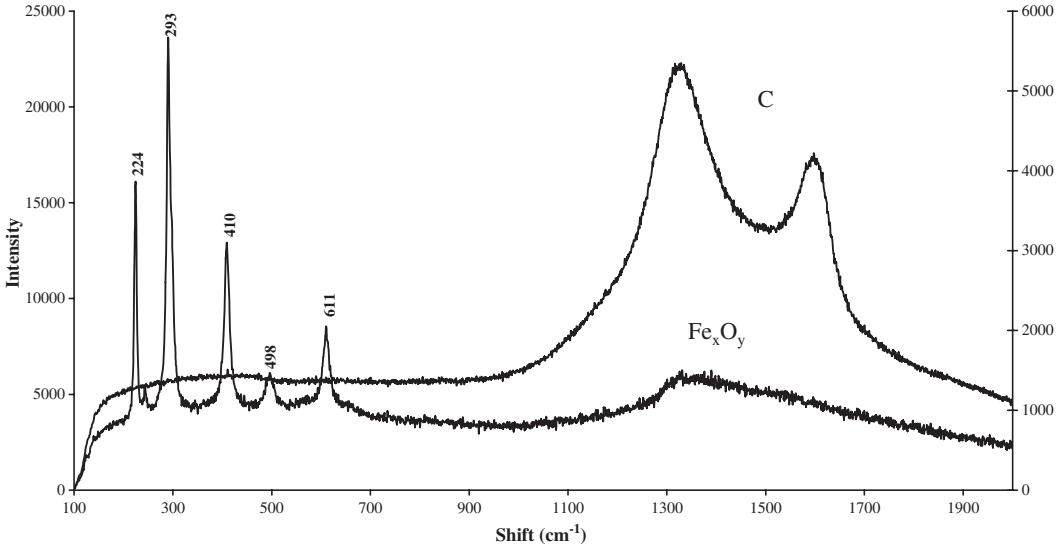

Fig. 7. Raman spectra of blast furnace slag obtained with the 785 nm excitation.

reported for the centre of a glass spherulite is even more comparable with the spectrum obtained for CS(2). It is therefore possible to speculate that the calcium silicate observed is a melilite. The various manganese oxides were also not identified in this analysis. Various forms of iron oxides were however identified.

4. Conclusions

The use of micro-Raman spectrometry provides spatial and spectral resolution that enables the identification of varying mineral phases in grey ordinary Portland cement, without any special preparation of the sample. Structural fluorescence as observed by Newman et al. [2] was not observed when the NIR laser (785 nm) was used in this configuration and identification of the various mineral phases was possible. Although the superior excitation wavelength range seems to be UV–VIS, with careful selection of measuring conditions, reasonable spectra could be obtained with both VIS and NIR lasers.

SCMs, by names the various forms of gypsum as found in cement or cementitious materials, fly ash and slag could be successfully characterized and the superior excitation wavelength proved to be 514.5 nm.

Raman chemical imaging and mapping could prove to be a valuable tool to describe the distribution of the various phases in various types of cements.

Acknowledgements

SSPV acknowledges the financial support from the FWO (Fund for Scientific Investigation, Flanders) and UA (University of Antwerp) for fellowships.

References

[1] J. Bensted, Cem. Concr. Res. 59 (1976) 140.
[2] S.P. Newman, S.J. Clifford, P.V. Coveney, V. Gupta, J.D. Blanchard, F. Serafin, D. Ben-Amotz, S. Diamond, Cem. Concr. Res. 35 (8) 1620.
[3] M. Conjeaud, H. Boyer, Cem. Concr. Res. 10 (1980) 61.
[4] D. Bonen, T.J. Johnson, S.L. Sarkar, Cem. Concr. Res. 24 (1994) 959.
[5] C.D. Dyer, P.J. Hendra, Spectrochim. Acta 49 (5/6) (1993) 715.
[6] S.S. Potgieter-Vermaak, J.H. Potgieter, R. Van Grieken, Cem. Concr. Res. (in press).
[7] L.K.A. Sear, Proceedings of the International Workshop on Novel Products from Combustion Residues: Opportunities and Limitations, Morella, Spain, 6-8 June, 2001, p. 47.
[8] B.E. Scheetz, W.B. White, in: McCarthy, R.J. Lauf (Eds.), Proceedings of MRS Conference on: Fly Ash and Coal Conversion By-Products: Characterization, Utilization and Disposal I, MRS, vol. 43, 1985, p. 53.
[9] B.E. Scheetz, W.B. White, F. Adar, in: R.L. Snyder, R.A. Condrate Sr., P.E. Johnson (Eds.), Advances in Materials Characterization: II, Materials Science Research, vol. 19, Plenum Press, 1985, p. 145.
[10] R.J. Kirkpatrick, J.L. Yarger, P.F. McMillan, P. Yu, X. Cong, Adv. Cem. Based Mater. 5 (1997) 93.
[11] A.G. Kalampounias, G.N. Papatheodorou, S.N. Yannopoulos, J. Non-Cryst. Solids 322 (2003) 35.
[12] C. Fredericci, E.D. Zanotto, E.C. Ziemath, J. Non-Cryst. Solids 273 (2000) 64.